Development 137, 1107-1116 (2010) doi:10.1242/dev.046045
© 2010. Published by The Company of Biologists Ltd

The RNA-binding protein bicaudal C regulates polycystin 2 in the kidney by antagonizing *miR-17* activity

Uyen Tran[1,*], Lise Zakin[2,*], Axel Schweickert[3], Raman Agrawal[1], Remziye Döger[1], Martin Blum[3], E. M. De Robertis[2] and Oliver Wessely[1,4,†]

SUMMARY

The RNA-binding protein Bicaudal C is an important regulator of embryonic development in *C. elegans*, *Drosophila* and *Xenopus*. In mouse, bicaudal C (*Bicc1*) mutants are characterized by the formation of fluid-filled cysts in the kidney and by expansion of epithelial ducts in liver and pancreas. This phenotype is reminiscent of human forms of polycystic kidney disease (PKD). Here, we now provide data that Bicc1 functions by modulating the expression of polycystin 2 (Pkd2), a member of the transient receptor potential (TRP) superfamily. Molecular analyses demonstrate that Bicc1 acts as a post-transcriptional regulator upstream of Pkd2. It regulates the stability of *Pkd2* mRNA and its translation efficiency. Bicc1 antagonized the repressive activity of the *miR-17* microRNA family on the 3′UTR of *Pkd2* mRNA. This was substantiated in *Xenopus*, in which the pronephric defects of *bicc1* knockdowns were rescued by reducing *miR-17* activity. At the cellular level, Bicc1 protein is localized to cytoplasmic foci that are positive for the P-body markers GW182 and HEDLs. Based on these data, we propose that the kidney phenotype in *Bicc1*$^{-/-}$ mutant mice is caused by dysregulation of a microRNA-based translational control mechanism.

KEY WORDS: P-bodies, Polycystic kidney disease, microRNA, Pronephros, Translational regulation, Mouse, *Xenopus*

INTRODUCTION

The vertebrate kidney is essential to conserve water, electrolytes and metabolites, as well as to remove metabolic waste products from the body. It develops through three successive and increasingly complex renal structures: the pronephros, mesonephros and metanephros (Saxén, 1987; Vize et al., 2002). These three kidney forms appear very different, but all rely on the same functional unit, the nephron. The structure and formation of the nephron is evolutionarily conserved (Mobjerg et al., 2000; Zhou and Vize, 2004; Dressler, 2006; Raciti et al., 2008). The kidney as a whole, and the nephron in particular, is an example of a tubular organ (Hogan and Kolodziej, 2002). As such, the kidney has attracted much attention in understanding how mesenchymal cells undergo the mesenchymal-epithelial transition (MET) to form the highly specialized renal tubules. In addition, the integrity of the tubules needs to be maintained throughout life to promote proper kidney function. In humans, the disruption of these processes results in a wide array of genetic diseases. Among these, polycystic kidney diseases (PKDs) are the leading cause of end-stage renal disease in children and adults (Torres and Harris, 2007; Wilson and Goilav, 2007). They are characterized by fluid-filled cysts that result from unregulated expansion of renal epithelial cells. The most frequent form of PKD, autosomal dominant PKD (ADPKD), is caused by mutations in *PKD1* and *PKD2* (Burn et al., 1995; Hughes et al., 1995; Mochizuki et al., 1996; The International Polycystic Kidney Disease Consortium, 1995). These genes encode polycystin 1 (PKD1; polycystic kidney disease 1), an 11-transmembrane-domain protein, and polycystin 2 (PKD2; polycystic kidney disease 2), a member of the transient receptor potential (TRP) superfamily. PKD1 and PKD2 are present in a cation channel complex that is involved in mechanosensation-triggered Ca^{2+} influx into cells. The second type of PKD, autosomal recessive PKD (ARPKD), is primarily caused by mutations in a single gene, *PKHD1*, which encodes a receptor-like membrane protein of unknown function known as polyductin, fibrocystin or tigmin (Hildebrandt et al., 1997; Onuchic et al., 2002; Ward et al., 2002; Xiong et al., 2002). Many animal models of PKD have been developed to better understand the process of cyst formation (Guay-Woodford, 2003; Drummond, 2005). Among these, mice with spontaneous mutations in the bicaudal C (*Bicc1*) locus are the least understood (Cogswell et al., 2003).

Bicc1 encodes an evolutionarily conserved RNA-binding molecule that consists of five N-terminal KH (hnRNP K homology) RNA-binding domains and a C-terminal protein-protein interaction SAM (sterile alpha motif) domain. *Bicaudal C* was originally identified in a *Drosophila* mutagenesis screen as a gene in which heterozygous females produced embryos with ‘double-abdomen’ phenotypes (Mohler and Wieschaus, 1986). Subsequent studies in both *Drosophila* and *C. elegans* suggest that Bicaudal C regulates mRNA stability and translation via modulation of mRNA polyadenylation (Mahone et al., 1995; Saffman et al., 1998; Wang et al., 2002; Suh et al., 2006; Chicoine et al., 2007). Previously, we identified the *Xenopus* and mouse homologs of Bicaudal C (Wessely and De Robertis, 2000; Wessely et al., 2001). Interestingly, *bicc1* is expressed in the renal epithelial cells of the *Xenopus* pronephros and loss of Bicc1 results in a PKD-like phenotype (Tran et al., 2007). Eliminating Bicc1 protein using antisense morpholino oligomers (MOs) impairs the physiological role of the pronephros by interfering with its osmoregulatory function, which leads to edema formation in the *Xenopus* embryo. At the molecular level, Bicc1 is required for the differentiation of renal cells of the late distal tubule and pronephric duct.

[1]Department of Cell Biology & Anatomy, [4]Department of Genetics, LSU Health Sciences Center, MEB 6A12, 1901 Perdido Street, New Orleans, LA 70112, USA. [2]HHMI, University of California, Los Angeles, Department of Biological Chemistry, 675 Charles E. Young Drive South, Los Angeles, CA 90024, USA. [3]University of Hohenheim, Institute of Zoology, Garbenstrasse 30, D-70593 Stuttgart, Germany.

*These authors equally contributed to this work
†Author for correspondence (owesse@lsuhsc.edu)

Accepted 20 January 2010

In mouse, *Bicc1* is expressed in the meso- and metanephric kidney (Wessely et al., 2001). Here, we now further investigate the biological role of Bicc1 by eliminating the gene using homologous recombination. The *Bicc1* mutant mice rarely survived postnatally and developed severe PKD. At birth, cysts were detected along the entire length of the nephron. Interestingly, the loss-of-function phenotype of *Bicc1* was remarkably similar to that of *Pkd2*. Experiments using the *Xenopus* pronephros, the mouse metanephric kidney and human HEK293T cells showed that both genes actually function in the same pathway, with Bicc1 acting upstream of *Pkd2*. Moreover, Bicc1 was localized to cytoplasmic foci that contain proteins involved in post-transcriptional regulation of mRNAs, and Bicc1 modulated Pkd2 protein levels by antagonizing microRNA (miRNA)-mediated repression within the 3′UTR of *Pkd2* mRNA.

MATERIALS AND METHODS

Gene targeting

The *Bicc1* mutation was performed by fusing the β-galactosidase (*lacZ*) gene with exon 4 of *Bicc1* and by deleting part of exon 4 and all of exons 5-8. Correct integration of the targeting construct was confirmed by Southern blot (see Fig. 1A for the position of the 5′ and 3′ probes). Electroporation and injection of the positive clones was performed by the ES Cell and Transgenic Core facilities at UCLA. Mice carrying the *Bicc1* mutation were backcrossed into the B6SJLF1/J hybrid strain (Jackson Laboratories) and all the experiments described here used the B6SJLF1/J hybrid.

Xenopus embryo manipulations

Xenopus embryos obtained by in vitro fertilization were maintained in 0.1× modified Barth medium (Sive et al., 2000) and staged according to Nieuwkoop and Faber (Nieuwkoop and Faber, 1994). The antisense MOs (GeneTools, LLC) used in this study were (5′ to 3′): *xBicC-MO1*, GGGACAAAGATGCTCATTTTAACAG; *xBicC-MO2*, GCCACTATCTCTTCAATCATCTCCG; *Pkd2-MO*, GGTTTGATTCTGCTGGGATTCATCG; and *miR-17-MO*, ACTACCTGCACTGTAAGCACTTTGA. Unless otherwise indicated, a total of 3.2 pmol of *Pkd2-MO*, *miR-17-MO* and *Std-MO* or a mixture of 3.2 pmol *xBicC-MO1* and 3.2 pmol *xBicC-MO2* (*xBicC-MO1+2*) was injected radially at the 2- to 4-cell stage into *Xenopus* embryos.

For synthetic mRNA, *pCS2-xBicC** (Tran et al., 2007), *pCS2-xBicC-GFP*, *pCS2-Pkd2* and *pCS2-Pkd2-myc* were linearized with *Not*I and transcribed with SP6 RNA polymerase. *pXEXβGal-Pkd2(short_UTR)* and *pXEXβGal-Pkd2(long_UTR)* were linearized with *Asp*718 and transcribed with T7 RNA polymerase using the mMessage mMachine (Ambion). For the synthetic *miR-17* duplex, two oligos (5′-rArCrCrUrGrCrArCrUrGrUrArArGrCrArCrUrUrUrGTT-3′ and 5′-rCrArArArGrUrGrCrUrUrArCrArGrUrGrCrArGrGrUAG-3′) were synthesized and annealed (Integrated DNA Technologies). Rescue experiments and miRNA reporter assays in *Xenopus* and HEK293T cells were performed as previously described (Tran et al., 2007; Agrawal et al., 2009).

In situ hybridization, immunohistochemistry, lectin staining and histology

Whole-mount and paraplast section in situ hybridizations were performed as previously described (Tran et al., 2007; Agrawal et al., 2009). The sequence of the LNA-modified *miR-17* degenerate oligomer is 5′-CTAC^{LNA}CTG^{LNA}CAC^{LNA}TRT^{LNA}DAG^{LNA}CAC^{LNA}TTT^{LNA}G-3′.

For immunohistochemistry and lectin staining, mouse kidneys were fixed in 4% paraformaldehyde and *Xenopus* embryos were fixed in Dent's fixative. The following antibodies/lectins were used: anti-acetylated α-tubulin (Sigma); peroxidase-conjugated *Dolichos biflorus* agglutinin (DBA, Sigma); anti-Pkd2 (Millipore); anti-phospho-histone H3 (Millipore); biotinylated *Lotus tetragonolobus* agglutinin (LTA, Vector Laboratories); anti-Nkcc2 (Slc12a1) (kind gift of Dr Mark Knepper, NIH); and anti-Pcna (DAKO). β-galactosidase staining was performed on cryostat sections or whole-mounts following the protocol described by Ma et al. (Ma et al., 2002) with minor modifications in the fixation timing. For histological staining, tissues were fixed in Bouin's Fixative and stained with Hematoxylin and Eosin (H&E), Periodic Acid Schiff (PAS) or Mallory's Tetrachrome.

RT-PCR and polyadenylation assay

Metanephric kidneys were processed for reverse transcription using standard protocols. Isolation of capped mRNA was performed using the mRNA-ONLY Eukaryotic mRNA Isolation Kit (Epicentre Biotechnologies). Conventional PCR for mouse *Bicc1* was performed using primers hBicC1 upper (5′-GGGTTGTCTTCCTCTTGTGT-3′) and hBicC1 lower (5′-AGAGTGAGTTTGGGGTTGTT-3′), which amplify a 377 bp fragment covering exons 9 to 11. Quantitative PCR was performed using the Applied Biosystems 7500 FAST Real-time PCR System and TaqMan Gene Expression Assays.

The length of the poly(A) tail of *Pkd2* mRNA was determined using RNA ligation-coupled RT-PCR (RL-PCR) as previously described (Charlesworth et al., 2004) using the *Pkd2* primer 5′-CTGGTAGTCTCCCCTCTGT-3′. To visualize the *Pkd2*-specific amplification products, the PCR reactions were separated on a 1% agarose gel and processed for non-radioactive Southern blotting using a *Pkd2*-specific probe.

Protein analysis

HEK293T cells were transfected using Lipofectamine 2000 (Invitrogen) following the manufacturer's instructions. Kidneys and HEK293T cells were lysed in T-PER Tissue Protein Extraction Reagent (Thermo Scientific) and processed for western blot analysis using standard protocols. For the subcellular localization studies, transfected HEK293T cells were cultured on Lab-TekII chamber slides (Nalgene Nunc) and processed for immunofluorescence analysis 48 hours post-transfection. Stress granule formation was studied in HeLa cells treated with 20 μM clotrimazole (Sigma) for 45 minutes in serum-free medium.

The following primary antibodies were used: anti-actin (Sigma); anti-calregulin (Santa Cruz); anti-Eif3η (Santa Cruz); anti-Eif4E (Santa Cruz); anti-GM130 (BD Biosciences); anti-GW182 (Abcam and Santa Cruz); anti-Lamp2 (DSHB); anti-Pkd2 (Santa Cruz); anti-Pkd2 (YCC2) (Markowitz et al., 1999); and anti-p70 S6 kinase-α [Rps6kb1; this antibody cross-reacts with HEDLs (Stoecklin et al., 2006); Santa Cruz].

RESULTS

Expression of bicaudal C in the kidney

Bicaudal C (Bicc1) has been shown to be mutated in two mouse models of PKD, *bpk* and *jcpk* (Cogswell et al., 2003). *bpk* mice, in particular, are widely used as a late onset model of PKD (Sweeney et al., 2000; Shillingford et al., 2006). However, the molecular mechanism of cyst formation by impaired Bicc1 function is still poorly understood. To address this, we generated a targeted mutation of *Bicc1* in mouse, in which parts of exon 4 were fused in frame to β-galactosidase, replacing exons 4-8 (Fig. 1A). The fusion protein lacks all known functional domains of Bicc1 (the RNA-binding KH domains and the protein-protein interaction SAM domain). Southern blot and RT-PCR analyses confirmed proper targeting of the *Bicc1* locus and the absence of alternatively spliced transcripts (Fig. 1B-D; see Fig. S1A in the supplementary material; data not shown), supporting the conclusion that these mice lack a functional Bicc1 protein.

To better understand the kidney phenotype of *Bicc1*$^{-/-}$ mice, we first analyzed the expression of *Bicc1* by in situ hybridization at different stages of kidney development. At embryonic day (E) 11.5, *Bicc1* mRNA was detected in the cranial and caudal tubules of the mesonephros, the Wolffian duct and the first branch of the ureteric bud (UB) tree (Fig. 1E; data not shown). Later, *Bicc1* was present in the UB tree, but was also found in renal vesicles and in the comma- and S-shaped bodies (Fig. 1F-H; data not shown). At E18.5, *Bicc1* mRNA was detected in all epithelial components of the kidney (Fig. 1I-K). *lacZ* staining faithfully recapitulated the expression of *Bicc1*

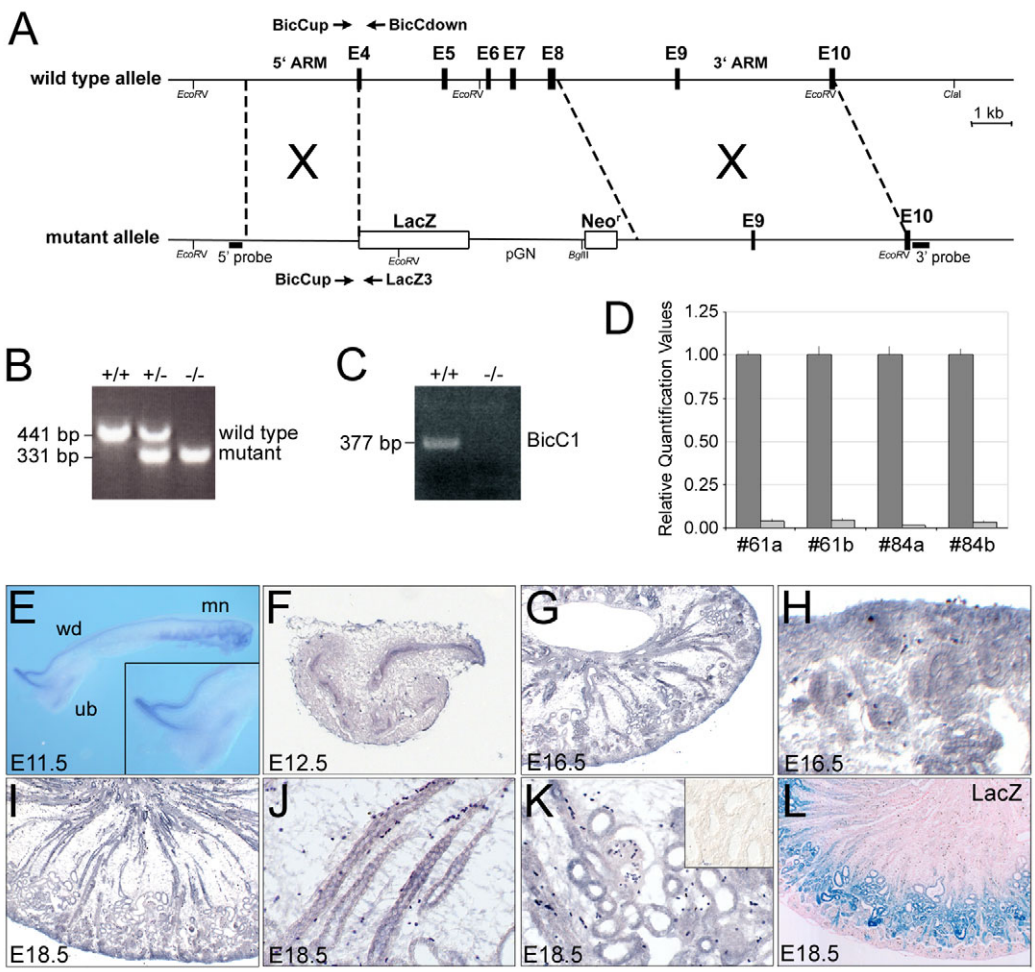

Fig. 1. Expression analysis and knockout of *Bicc1* in mouse. (**A**) Schematic of *Bicc1* loss-of-function strategy. (**B**) PCR-based genotyping of *Bicc1* mice. (**C**) RT-PCR for *Bicc1* in kidneys from *Bicc1*$^{+/+}$ and *Bicc1*$^{-/-}$ mice using primers spanning exons 9 to 11. (**D**) qPCR analysis of *Bicc1* expression using primers covering exons 15 and 16. Each of the four sets represents a comparison of a *Bicc1*$^{+/+}$ (dark gray) and a *Bicc1*$^{-/-}$ mutant (light gray) littermate. (**E**) Expression of *Bicc1* mRNA in the Wolffian duct (wd), mesonephros (mn) and T-stage branching of the metanephros (ureteric bud, ub) at E11.5. Inset is a magnified view of the ureteric bud. (**F-K**) In situ hybridization on paraplast sections of metanephric kidneys at E12.5 (F), E16.5 (G) and E18.5 (I) and magnified views of the nephrogenic zone at E16.5 (H), and of the collecting ducts (J) and glomeruli and proximal tubules (K) at E18.5. Inset in K shows sense control. (**L**) *lacZ* staining of an E18.5 *Bicc1*$^{+/-}$ kidney section counterstained with Eosin.

mRNA at early stages of development in the posterior notochord/ventral node and the developing endoderm (see Fig. S1B-C′ in the supplementary material) (Wessely et al., 2001; Blum et al., 2007). However, in the kidney, β-galactosidase activity was mainly observed in the proximal tubules at E18.5 (Fig. 1L). This discrepancy was probably due to reduced stability of the Bicc1-β-galactosidase fusion protein as the *lacZ* mRNA pattern was indistinguishable from that of *Bicc1* mRNA in the kidneys of *Bicc1*-heterozygous mice (see Fig. S1D,D′ in the supplementary material).

Polycystic kidney disease phenotype in *Bicc1*$^{-/-}$ mice

Bicc1 heterozygous intercrosses showed a lower than expected ratio of homozygous mutant progeny (see Table S1 in the supplementary material). The lethality of *Bicc1*$^{-/-}$ mice increased during development. Although Mendelian ratios were observed in embryos up to E14.5, more than half of the mutant mice died perinatally, for unknown reasons. Similar to *bpk* and *jcpk* mice (Nauta et al., 1993; Flaherty et al., 1995), surviving *Bicc1*$^{-/-}$ mice developed severely enlarged kidneys on both sides, caused by dramatic polycystic malformations (Fig. 2A,B,I). Cells lining the cysts lost their cuboidal shape and adopted a squamous appearance (Fig. 2D,F). Despite the increased size of the mutant kidneys, the nephrogenic zone was reduced (Fig. 2A,B). These mice also developed cysts in the bile ducts of the liver and the excretory ducts of the pancreas (see Fig. S2 in the supplementary material). In PKD, cysts arise from different segments of the nephron. To identify the origin of cysts in *Bicc1*$^{-/-}$ mice, segment-specific markers were analyzed. As shown in Fig. 2C-H, cysts at birth [post-natal day (P) zero, P0] were derived from glomeruli, proximal tubules and, to a lesser extent, from the thick ascending limb of the loop of Henle and collecting ducts. When *Bicc1*$^{-/-}$ kidneys were analyzed at earlier stages, cysts were first detected at E15.5. At this stage, cysts were mainly of glomerular origin, but extended towards more distal segments in subsequent stages (see Fig. S3 in the supplementary material). Interestingly, the early phase of cyst formation was not caused by uncontrolled proliferation. No obvious changes in proliferation were detected using antibodies against phospho-histone H3 and proliferating cell nuclear antigen (Pcna) (see Fig. S4 in the supplementary material). In agreement with the observations made in mouse, the PKD-like phenotype of *Xenopus* embryos lacking Bicc1 protein (Tran et al., 2007) was not due to defects in proliferation (data not shown).

Bicc1 regulates Pkd2

In humans, PKD is caused primarily by mutations in *PKD1*, *PKD2* and *PKHD1* (Torres and Harris, 2007; Wilson and Goilav, 2007). To determine whether the loss of Bicc1 affected any of these genes, we performed quantitative PCR (qPCR) analysis using multiple kidneys, comparing *Bicc1*$^{+/+}$ with *Bicc1*$^{-/-}$ littermates at E15.5 and E18.5. As shown in Fig. 3A-C, *Pkd2* mRNA was significantly downregulated in *Bicc1*$^{-/-}$ kidneys, whereas no significant changes were detected for *Pkd1* or *Pkhd1*. This effect was stage dependent, as the downregulation of *Pkd2* mRNA was more pronounced at E18.5. Western blot analyses comparing kidneys from *Bicc1*$^{+/+}$,

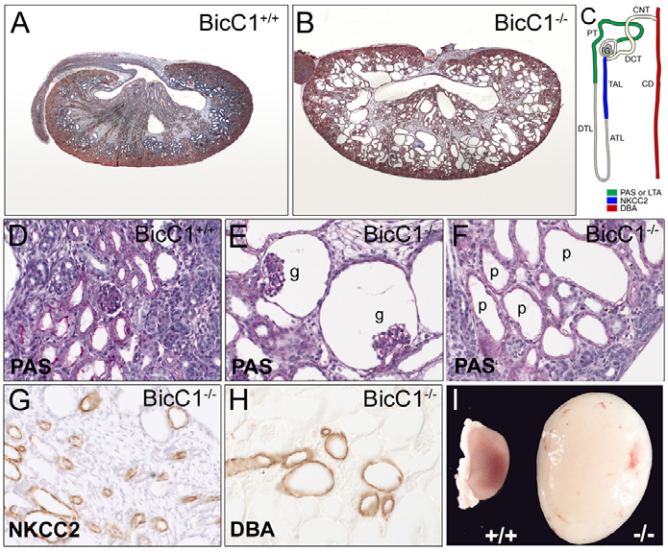

Fig. 2. Polycystic kidney disease (PKD) phenotype in *Bicc1*$^{-/-}$ mice. (**A**,**B**) Mallory's Tetrachrome staining on *Bicc1*$^{+/+}$ (A) and *Bicc1*$^{-/-}$ (B) littermates at P0. (**C**) Schematic of a nephron indicating the localization of the segment-specific markers shown in D-H. ATL, ascending thin limb of Henle's loop; CD, collecting duct; CNT, connecting tubule; DCT, distal convoluted tubule; DTL, distal thin limb or Henle's loop; G, glomerulus; PT, proximal tubule; TAL, thick ascending limb of Henle's loop. (**D-F**) Periodic Acid Schiff (PAS) staining of *Bicc1*$^{+/+}$ (D) and *Bicc1*$^{-/-}$ (E,F) kidneys showing glomerular (g) and proximal tubule (p) cysts at P0. (**G**,**H**) Immunohistochemistry on sections of kidneys from P0 mutant mice using an Nkcc2 antibody and *Dolichos biflorus* agglutinin (DBA). (**I**) Morphology of a *Bicc1*$^{-/-}$ cystic kidney compared with a *Bicc1*$^{+/+}$ littermate at P21.

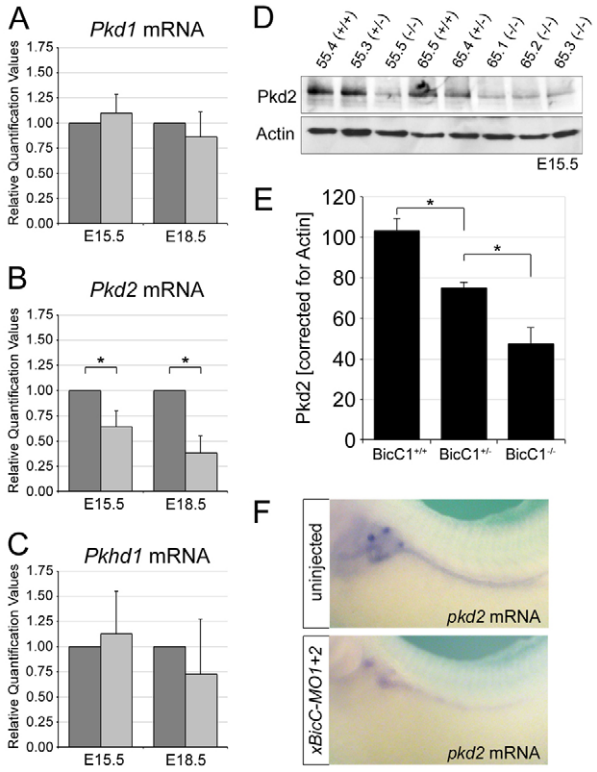

Fig. 3. Bicc1 regulates Pkd2. (**A-C**) qPCR analysis for mouse *Pkd1*, *Pkd2* and *Pkhd1* mRNA levels in *Bicc1*$^{+/+}$ (dark gray) and *Bicc1*$^{-/-}$ (light gray) littermates. The averages and s.d. from six kidney pairs at E15.5 and four pairs at E18.5 are shown (*, $P<0.05$, Student's *t*-test). (**D**) Western blot analysis comparing Pkd2 protein levels in E15.5 kidneys from two *Bicc1* mouse litters (#55 and #65) of the indicated genotypes using the Pkd2-specific antibody from Santa Cruz. Actin served as a loading control. (**E**) Quantification of multiple Pkd2 western blot analyses comparing several mouse litters at E15.5 and normalized to actin. Average values and s.d. are indicated (*, $P<0.05$, Student's *t*-test). (**F**) Whole-mount in situ hybridization for *Pkd2* mRNA on uninjected and *xBicC-MO1+2*-injected *Xenopus* embryos at stage 39.

Bicc1$^{+/-}$ and *Bicc1*$^{-/-}$ littermates at E15.5, i.e. at the onset of cyst development, showed a dramatic decrease in Pkd2 protein levels (using two different antibodies; Fig. 3D,E and see Fig. S8A in the supplementary material). Interestingly, this reduction was dose dependent, as heterozygous kidneys also had lower amounts of Pkd2 compared with the wild type.

To explore the significance of this observation, we turned to *Xenopus*, in which the loss of Bicc1 results in a PKD-like phenotype (Tran et al., 2007). In *Xenopus*, *pkd2* mRNA and protein were expressed in all renal epithelial cells of the pronephros (Fig. 3F; see Fig. S5A-C″ in the supplementary material), a pattern identical to that of *bicc1* (Tran et al., 2007). As shown in Fig. 3F, the expression of *pkd2* mRNA was significantly reduced in the absence of Bicc1 protein, demonstrating that the regulation of Pkd2 by Bicc1 is evolutionarily conserved.

Epistasis analysis between Bicc1 and Pkd2 in the *Xenopus* pronephros

In addition to these molecular observations, the phenotype of *Bicc1*$^{-/-}$ embryos is similar to that of *Pkd2* mutants (Wu et al., 2000; Pennekamp et al., 2002). *Bicc1*$^{-/-}$ mice showed kidney, liver and pancreatic cysts (Fig. 2; see Fig. S2 in the supplementary material), as well as defects in left-right patterning (data not shown). Therefore, we decided to test the interaction between Bicc1 and Pkd2 using the *Xenopus* pronephric kidney. Knockdown of *Xenopus* Pkd2 protein with an antisense MO (*Pkd2-MO*) resulted in a PKD-like phenotype highly reminiscent of that observed in embryos lacking Bicc1 (Tran et al., 2007) (see Figs S5-S7 in the supplementary material). These defects are specific as they were not seen in embryos that were microinjected with a standard control MO (Tran et al., 2007) (data not shown). In addition, the expression of *nbc-1* in the late distal tubule was rescued by co-injection of *pkd2-myc* mRNA (see below, Fig. 4D).

Next, we examined the epistatic relationship between Bicc1 and Pkd2. We asked whether *pkd2* mRNA could rescue the effects of *xBicC-MO1+2* injections and vice versa, i.e. whether *bicc1* mRNA could rescue the effects of *Pkd2-MO* injections. We followed the same strategy described by Tran et al. (Tran et al., 2007), assaying for the expression of *nbc-1* in the late distal tubule by in situ hybridization. Although this paradigm represents only part of the PKD-like phenotype, it provides a powerful readout to quantitatively assess Bicc1 and Pkd2 function in the pronephros. We categorized embryos into those with bilateral expression of *nbc-1* in the late distal tubule, those with reduced expression and those with unilateral expression rescued by the co-injected mRNA. *Xenopus* embryos were radially injected at the 2-cell stage with either *xBicC-MO1+2* or *Pkd2-MO*. At the 4-cell stage, a subset of these embryos was then injected with either *pkd2* or *bicc1* mRNA into a single blastomere. Embryos were grown until stage 39 and processed for whole-mount

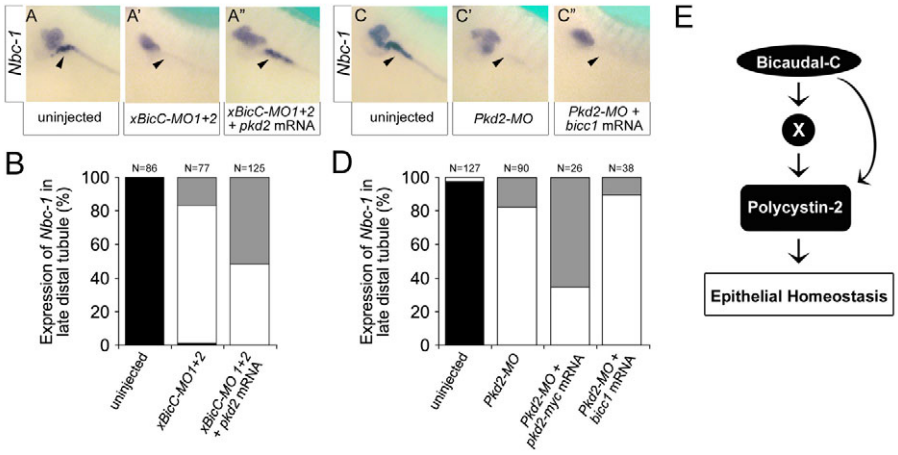

Fig. 4. Bicc1 is epistatic to Pkd2. (**A-A″**) Analysis of the expression of *nbc-1* in the *Xenopus* late distal tubule at stage 39 by whole-mount in situ hybridization of uninjected control embryos, and embryos radially injected with *xBicC-MO1*+2 in the presence or absence of a single injection of 2 ng *pkd2* mRNA. (**B**) Quantification of the expression of *nbc-1* in the late distal tubule from the experiments shown in A-A″. Black, bilateral expression; white, no expression; gray, unilateral expression rescued by co-injected mRNA. The number of embryos analyzed is indicated. (**C-D**) Reciprocal experiments to those in A-B using *Xenopus* embryos injected with either *Pkd2-MO* alone or together with *pkd2-myc* or *bicc1* mRNA. Co-injection with *pkd2-myc* rescued *nbc-1* expression, whereas co-injection with *bicc1* did not. (**E**) Flow diagram outlining the proposed mechanism of Bicc1 activity.

in situ hybridization for *nbc-1* mRNA. As previously observed (Tran et al., 2007), *nbc-1* expression in the late distal tubule was lost upon injection of *xBicC-MO1+2* (Fig. 4A,A′,B). When *pkd2* mRNA was injected, the expression of *nbc-1* was restored on the injected side in 52% of cases (Fig. 4A″,B). Interestingly, in the reciprocal experiment, *bicc1* mRNA was unable to rescue the effects of the injected *Pkd2-MO*, whereas a *pkd2* mRNA construct (*pkd2-myc*) that is not targeted by the *Pkd2-MO* did rescue this expression domain (Fig. 4C-D).

Together, these data suggested that Bicc1 acts upstream of Pkd2 and is necessary for Pkd2 activity. Based on these observations, we propose that either the *Pkd2* mRNA itself, or a gene that regulates its expression, is a target for Bicc1 activity (Fig. 4E). In the absence of Bicc1, the spatiotemporal regulation of Pkd2 is disturbed, but not completely disrupted.

Subcellular localization of Bicc1

In order to understand the molecular mechanism of Bicc1, we next studied its subcellular localization. We used a *Xenopus* Bicc1-GFP fusion construct (xBicC-GFP) that has the same biological activity as its untagged counterpart, i.e. it induces ectopic endoderm formation in whole embryos and *endodermin* mRNA in ectodermal explants (see Fig. S8B in the supplementary material; data not shown) (Wessely and De Robertis, 2000). mRNA encoding xBicC-GFP was microinjected into the animal pole of *Xenopus* embryos and analyzed by fluorescence microscopy at gastrula stage (Fig. 5A,B). The protein was not nuclear, but was instead detected in cytoplasmic foci of unknown identity. To further investigate this localization, the xBicC-GFP fusion protein was transfected into HEK293T cells and analyzed by immunofluorescence 48 hours later. xBicC-GFP localization was compared with staining by a panel of antibodies that recognize subcellular cytoplasmic compartments: the Golgi apparatus (GM130; Golga2), endoplasmic reticulum (calregulin; calreticulin) and lysosomes (Lamp2). As shown in Fig. 5C-E, xBicC-GFP did not colocalize with any of these proteins, suggesting that it is not part of these structures.

Another structure that appears as distinct cytoplasmic foci are the so-called ‘processing bodies’ (P-bodies, or GW-bodies) (Parker and Sheth, 2007). Interestingly, immunofluorescence using antibodies against two components of these foci, GW182 (Tnrc6a) and HEDLs (Edc4) (Kedersha and Anderson, 2007), showed overlapping expression with the xBicC-GFP foci (Fig. 5F-G″). This colocalization was confirmed in multiple cell lines (IMCD3, LLC-PK1, MDCK and HeLa), as well as with two additional constructs: Flag-tagged *Xenopus* Bicc1 and a mouse Bicc1-GFP fusion protein (Fig. 5H-I; data not shown).

P-bodies are closely related to a second class of RNA granules known as stress granules. These are normally not present in cells, but are induced under adverse conditions to halt mRNA metabolism and are dynamically linked to P-bodies (Anderson and Kedersha, 2008). To explore whether Bicc1 is also found in stress granules, HeLa cells were transfected with xBicC-GFP. Stress granule formation was induced by the addition of clotrimazole and visualized by immunofluorescence using antibodies against Eif3η (Eif3B; which stains only stress granules) and Eif4E (which stains P-bodies and stress granules). Under these conditions, xBicC-GFP was found in large aggregates that were positive for these stress granule markers (Fig. 5I-J‴). Based on these results, we conclude that Bicc1 is a component of the cytoplasmic mRNA metabolism machinery.

Bicc1 is a post-transcriptional regulator

GW182 protein has been shown to be involved in mRNA degradation, stability, polyadenylation and miRNA activity (Parker and Sheth, 2007). To study whether Bicc1 regulates Pkd2 levels via such mechanisms, we first re-evaluated the qPCR and western blot data from the *Bicc1* mouse kidneys (Fig. 3B,D,E; data not shown). The average decrease in *Pkd2* mRNA levels, comparing six independent pairs of E15.5 kidneys from $Bicc1^{+/+}$ and $Bicc1^{-/-}$ littermates, was 29% (Fig. 6A). Similar calculations for Pkd2 protein levels from seven independent pairs showed a 54% decrease (Fig. 3E). When analyzed in this manner, Pkd2 protein levels were more substantially decreased than mRNA

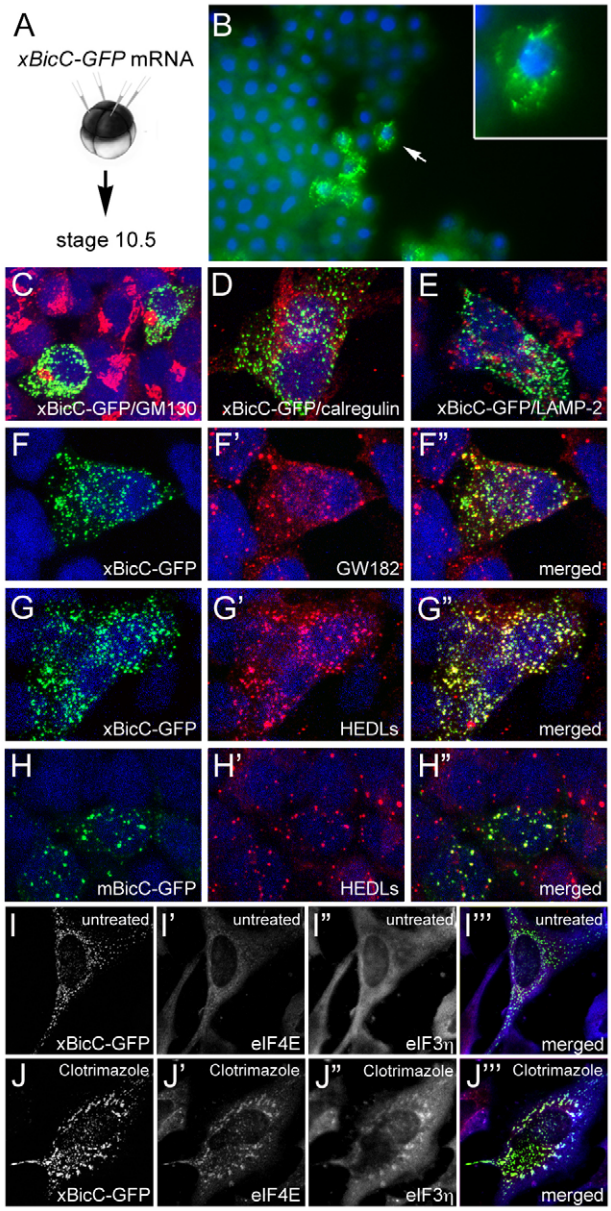

Fig. 5. Subcellular localization of Bicc1. (**A**,**B**) mRNA encoding a *Xenopus* Bicc1-GFP fusion protein (xBicC-GFP) was injected into the animal region of *Xenopus* embryos and analyzed at gastrula stage by immunofluorescence microscopy. Inset is a magnified view of a single cell (arrow). (**C-H″**) HEK293T cells were transfected with plasmids encoding xBicC-GFP (C-G″) or a mouse Bicc1-GFP fusion protein (mBicC-GFP; H-H″) and processed for immunofluorescence with antibodies against GM130 (C), calregulin (D), Lamp2 (E), GW182 (F-F″) and HEDLs (G-H″), using red fluorescent secondary antibodies. Nuclei were counterstained with DAPI (blue). (**I-J‴**) HeLa cells were transfected with *pCS2-xBicC-GFP* and were either left untreated (I-I‴) or treated with 20 μM clotrimazole (J-J‴). Stress granule formation was visualized with antibodies against Eif4E (red) and Eif3η (blue). Note that even in the untreated cells, xBicC-GFP is partially colocalized with Eif4E, which is a marker for P-bodies and stress granules.

levels. Post-transcriptional regulation is often accompanied by mRNA degradation and is preceded by changes in the level of translationally active capped mRNA. To distinguish between total and capped mRNA, a 5′-phosphate-dependent exonuclease was used to degrade non-capped RNAs. qPCR analysis of these samples demonstrated that in *Bicc1*$^{-/-}$ kidneys, the reduction in the percentage of capped *Pkd2* mRNA was greater than that in total *Pkd2* mRNA (Fig. 6A). As with total mRNA (Fig. 3B, Fig. 6A), the reduction in capped *Pkd2* mRNA in *Bicc1*$^{-/-}$ kidneys was stage dependent. The differences at E15.5 were rather modest, whereas those at E18.5 were very pronounced. This effect was not accompanied by changes in the polyadenylation of *Pkd2* mRNA. RNA ligation-coupled RT-PCR (RL-PCR) (Charlesworth et al., 2004) did not detect any obvious differences in the length of the poly(A) tail of *Pkd2* mRNA in *Bicc1*$^{+/+}$ and *Bicc1*$^{-/-}$ mouse kidneys at E15.5 (Fig. 6B).

Since neither capping nor polyadenylation of *Pkd2* mRNA was significantly changed at E15.5, i.e. at the onset of cyst formation, we next asked whether overexpression of Bicc1 could directly increase the translation of *Pkd2* mRNA. Post-transcriptional regulation normally resides within the 3′UTR of a given mRNA. Interestingly, two different variants of the *Pkd2* 3′UTR could be found in databases: a long UTR corresponding to the published full-length *Pkd2* sequence (GenBank NM_008861) and a shorter one that lacks 1.3 kb in the middle of the 3′UTR (GenBank BC062969), presumably owing to alternative splicing (Fig. 6C). Plasmids containing both *Pkd2* variants were transfected into HEK293T cells in the presence or absence of *Xenopus* Bicc1 and processed for western blot analysis. As shown in Fig. 6D-F, Bicc1 significantly increased the amount of Pkd2 protein. This increase required the RNA-binding domain of Bicc1 because a construct lacking the KH domains (*xBicCΔKH*) did not show such an effect (Fig. 6D; see Fig. S9C in the supplementary material). It also required the 3′UTR of *Pkd2* because a construct completely lacking the 3′UTR (*Pkd2_noUTR*) was resistant to the activity of Bicc1 (Fig. 6E,F′).

Bicc1 protein colocalized with GW182 (Fig. 5F-F″), and GW182 is a crucial component in the regulation of mRNA translation and stability via miRNAs (Liu et al., 2005; Rehwinkel et al., 2005). Thus, it seemed plausible that the regulation of Pkd2 by Bicc1 involved miRNAs. To explore this, the 3′UTR of *Pkd2* mRNA was analyzed for potential miRNA binding sites using TargetScan (Version 5.0), PicTar and DIANA microT (version 3.0). As shown in Fig. 6C, two evolutionarily conserved miRNA binding sites, one for the *miR-17* family and one for *miR-194*, were detected. However, the short 3′UTR of *Pkd2* only contained a *miR-17* binding site. Even though we do not have any evidence that a *Pkd2* mRNA with the short 3′UTR exists in vivo, the fact that this construct was still regulated by Bicc1 (Fig. 6E,F) suggests that Bicc1 acts via the *miR-17* family. In situ hybridization using a degenerate locked nucleic acid (LNA)-modified oligomer that recognizes three members of the *miR-17* family (*miR-17*, *miR-20b* and *miR-106a*) detected expression in the mouse metanephric kidney at E14.5 and P0 and in the *Xenopus* pronephros (see Fig. S9A-C in the supplementary material). To assess whether this *miR-17* binding site in the 3′UTR of *Pkd2* was functional, two assays were performed. First, HEK293T cells were transfected with *Pkd2(miR-17mut)*, a construct in which the seed sequence of the *miR-17* binding site is mutated so that it does not bind *miR-17* (Fig. 6C). This construct, in contrast to its non-mutated counterpart, no longer showed any regulation of Pkd2 protein by Bicc1 (Fig. 6E,F″). Moreover, the mutated construct had a consistently higher baseline expression of Pkd2 (Fig. 6E, compare lanes 1 and 5), arguing that this *miR-17* binding site plays a role in the modulation of Pkd2 expression in HEK293T cells.

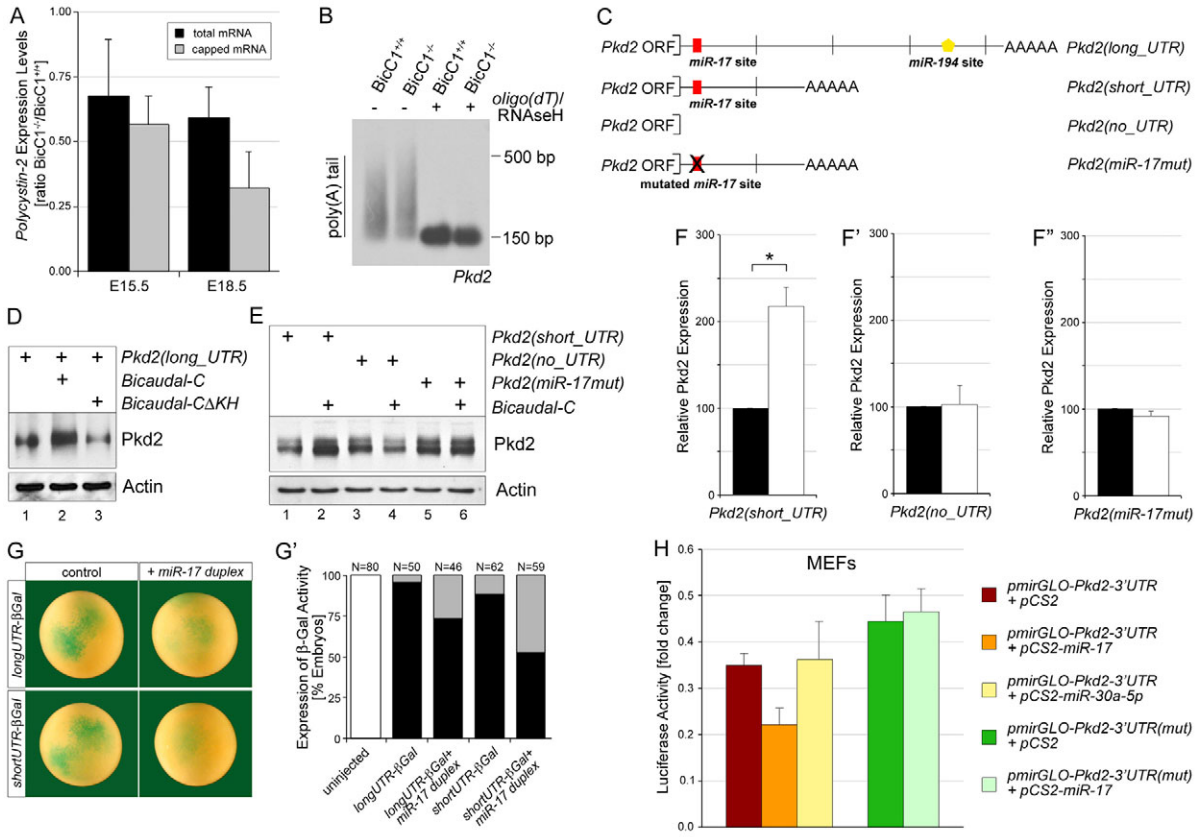

Fig. 6. Post-transcriptional regulation by Bicc1. (**A**) qPCR analysis of the reduction in *Pkd2* mRNA in the kidneys of *Bicc1*$^{+/+}$ and *Bicc1*$^{-/-}$ mouse littermates, comparing total and capped mRNA at E15.5 and E18.5. (**B**) RL-PCR to determine the length of the poly(A) tail of *Pkd2* mRNA, comparing kidneys of *Bicc1*$^{+/+}$ and *Bicc1*$^{-/-}$ littermates at E15.5. As a control for the specificity of the reaction, oligo(dT) and RNase H were added to remove the poly(A) tail before the RL-PCR, which collapsed the smear seen in the gel into a distinct band. (**C**) Schematic representation of *Pkd2* constructs [*Pkd2(long_UTR)*, *Pkd2(short_UTR)*, *Pkd2(no_UTR)*, *Pkd2(miR-17mut)*]. Predicted conserved miRNA binding sites are indicated. (**D**,**E**) Western blot of Pkd2 expression in HEK293T cells transfected with the four *Pkd2* constructs together with an empty vector control, *Xenopus bicc1* or a *bicc1* construct lacking the RNA-binding KH domains (*xBicCΔKH*). Equal loading was confirmed by actin. (**F-F″**) Quantification of three independent western blots showing mean values and s.d. (*, P<0.05). (**G**,**G′**) *Xenopus* embryos were injected with an mRNA containing the *lacZ* gene fused to the short or long 3′UTR of *Pkd2* in the presence or absence of a *miR-17* duplex and stained for *lacZ* expression at stage 10 (G). Multiple experiments were quantified and the number of embryos analyzed is indicated (G′). White, no *lacZ* staining; black, strong *lacZ* staining; gray, reduced *lacZ* staining. (**H**) Luciferase reporter assay of mouse embryonic fibroblasts (MEFs) transfected with *pmirGLO-Pkd2-3′UTR* and *pmirGLO-Pkd2-3′UTR-mut* in the presence of *pCS2*, *pCS2-miR-17* or *pCS2-miR-30a-5p*. Values were corrected for the expression of *Renilla* luciferase and calculated as fold change compared with the *pCS2* control. Multiple independent experiments were averaged and the s.d. is indicated (P<0.05).

Secondly, to test whether the putative *miR-17* binding site is responsive to *miR-17*, the long and short 3′UTRs of *Pkd2* were fused to a nuclear β-galactosidase gene (*nlacZ*). Synthetic mRNA of these constructs was injected into the animal region of *Xenopus* embryos in the absence or presence of a synthetic *miR-17* duplex. Embryos were processed for β-galactosidase staining at stage 10. The 3′UTR constructs in the absence of the *miR-17* duplex showed strong *lacZ* staining (Fig. 6G,G′). Co-injection of the *miR-17* duplex significantly reduced this staining. To quantify these *miR-17* effects, mouse embryonic fibroblasts (MEFs) were transfected with a dual luciferase reporter construct that harbors the 3′UTR of *Pkd2* (*pmirGLO-Pkd2-3′UTR*) in the presence or absence of *miR-17*, or, as control, *miR-30a-5p* (*pCS2-miR-17*, *pCS2-miR-30a-5p*). As shown in Fig. 6H, *miR-17* reduced luciferase expression by 37%, whereas *miR-30a-5p* did not have any repressive effect. Moreover, this repression was specific, as no effect was observed when the *miR-17* binding site was mutated (*pmirGLO-Pkd2-3′UTR-mut*).

Bicc1 and *miR-17*

The experiments described above supported the hypothesis that Bicc1 acts as a post-transcriptional regulator of *Pkd2* mRNA via its *miR-17* binding site. However, the *miR-17* duplex, as also seen with other miRNAs (Filipowicz et al., 2008), reduced the expression of the *Pkd2* 3′UTR reporters (Fig. 6G,G′), whereas Bicc1 increased it (Fig. 6D-F). Thus, a more logical interpretation of our data is that Bicc1 actually releases the repression by *miR-17* (Fig. 7D,D′). This was not due to changes in *miR-17* levels in *Bicc1* mutants. qPCR analyses of representative *miR-17* family members (corresponding to the three different primary transcripts) did not detect any differences in expression levels between *Bicc1*$^{+/+}$ and *Bicc1*$^{-/-}$ kidneys (data not shown). This argued that Bicc1 and *miR-17* both converge on the *Pkd2* transcript. We tested this hypothesis using the PKD-like phenotype in *Xenopus* as a paradigm. *miR-17* activity was knocked down using an antisense MO that targets several members of the *miR-17* family (*miR-17-MO*, Fig. 7A). *Xenopus* embryos were injected with *xBicC-*

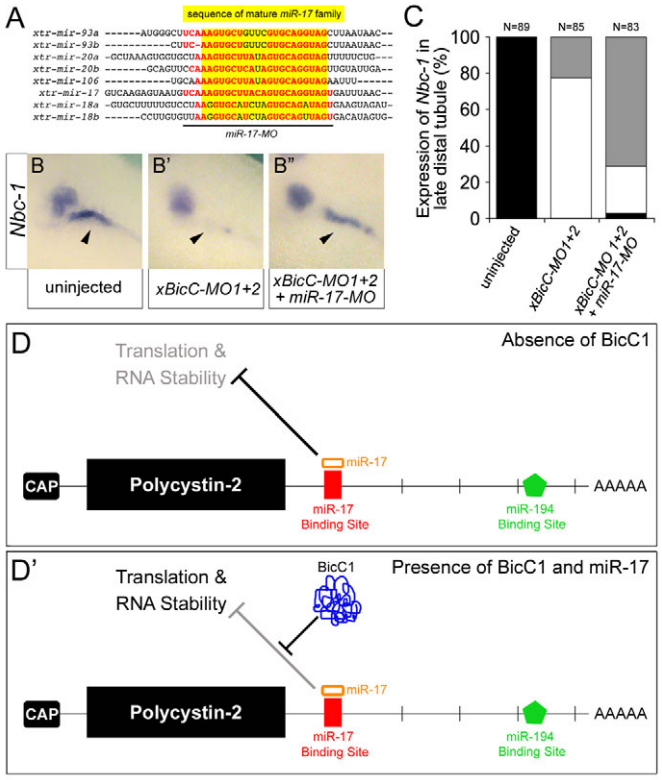

Fig. 7. Cross-talk between Bicc1 and the *miR-17* miRNA family. (**A**) Alignment of the *Xenopus miR-17* family members. Mature forms are highlighted in yellow. The sequence targeted by the *miR-17* antisense MO (*miR-17-MO*) is indicated by the black line. The nucleotides shared between *miR-17-MO* and the individual members are indicated in red. (**B-B″**) Analysis of the expression of *nbc-1* by whole-mount in situ hybridization of uninjected control embryos, embryos injected with *xBicC-MO1+2* alone or with *miR-17-MO*. Arrowheads indicate the expression of *nbc-1* in the *Xenopus* late distal tubule. Note that this expression domain is rescued upon co-injection of the two antisense MOs. (**C**) Quantification of the experiments shown in B-B″. Black, bilateral expression; white, reduced or no expression; gray, unilateral, rescued expression in the late distal tubule. (**D**,**D′**) Models for the post-transcriptional regulation of *Pkd2* mRNA by the *miR-17* family in the absence or presence of Bicc1.

MO1+2 alone, or together with *miR-17-MO*, and assayed for *nbc-1* expression in the late distal tubule by in situ hybridization. *bicc1* morphants lost *nbc-1* (Fig. 7B,B′,C), whereas *miR-17-MO* had no effect on *nbc-1* expression (data not shown). However, upon simultaneous reduction of *miR-17* and Bicc1 activity, *nbc-1* mRNA levels were recovered in 50% of the embryos (Fig. 7B″,C). This suggested that the *miR-17* family acted either downstream of, or parallel to, Bicc1, further supporting the proposed model (Fig. 7D,D′).

Together, the fact that the *miR-17* family is expressed in the kidney and that *Pkd2*, a gene with a *miR-17* binding site, is affected by Bicc1, support the hypothesis that Bicc1 is part of a post-transcriptional regulatory complex that is involved in epithelial homeostasis and which, when disrupted, leads to PKD.

DISCUSSION

Bicaudal C has been shown to be an important developmental regulator in *Drosophila*, *Xenopus*, *C. elegans* and mouse (Mahone et al., 1995; Saffman et al., 1998; Wessely and De Robertis, 2000; Wang et al., 2002; Cogswell et al., 2003; Suh et al., 2006; Tran et al., 2007; Maisonneuve et al., 2009). Here, we extend previous studies that showed that Bicc1 is required for the proper development of the mouse metanephric kidney (Cogswell et al., 2003). Loss of Bicc1 resulted in renal cyst formation. These cysts were initially located in the glomerulus and the proximal tubules, but were later found along the entire length of the nephron. This phenotype is reminiscent of human forms of PKD and adds to the existing animal models for PKD (Guay-Woodford, 2003; Torres and Harris, 2007). However, the molecular nature of the cystic phenotype in *Bicc1* mutant mice remained obscure. Based on the following observations, we now propose that Bicc1 functions as a post-transcriptional regulator of Pkd2. (1) The *Bicc1* and *Pkd2* mouse knockout phenotypes both result in the formation of cysts in the kidney, pancreas and liver, as well as in defects in left-right asymmetry (this study, data not shown) (Wu et al., 2000; Pennekamp et al., 2002). (2) Mice lacking a functional Bicc1 protein show reduced expression levels of Pkd2 mRNA and protein. (3) *Xenopus* embryos lacking Pkd2 develop a PKD-like phenotype that is highly reminiscent of that of embryos lacking Bicc1 (Tran et al., 2007). (4) *pkd2* mRNA rescues the effects of *bicc1* knockdown in *Xenopus*, but *bicc1* mRNA does not rescue *pkd2* morphants. (5) Bicc1 enhances the translation of *Pkd2* mRNA in HEK293T cells. (6) Bicc1 protein colocalizes with proteins that are involved in the post-transcriptional regulation of mRNAs. (7) *Pkd2* mRNA contains a binding site for the *miR-17* miRNA family in its 3′UTR, and knockdown of *miR-17* can rescue the phenotype of *bicc1* morphants in *Xenopus*.

One of the most revealing aspects of this study was the realization that Bicc1 is not localized to the nucleus, but acts as a post-transcriptional regulator in the cytoplasm (Fig. 5) (Maisonneuve et al., 2009; Stagner et al., 2009). The protein was localized to cytoplasmic foci that also contain proteins known to be involved in cytoplasmic mRNA turnover and was recruited to stress granules upon treatment with clotrimazole. It is noteworthy that the number of Bicc1-positive foci was much higher than the number of P-bodies detectable in HEK293T cells. Thus, whether Bicc1 is a bona fide P-body protein or whether it is a part of a more specialized subset of the cytoplasmic mRNA maintenance machinery remains to be determined. In particular, it will be important to verify the subcellular localization of the endogenous protein. However, one tempting speculation is that Bicc1 is part of the submicroscopic P-body subcomplex that has recently been described (Franks and Lykke-Andersen, 2007). The implications from the subcellular localization of Bicc1 are in agreement with data concerning its function in invertebrates. In *C. elegans*, GLD-3, a homolog of Bicaudal C, has been shown to act as a translational regulator by functioning as a specificity subunit for the cytoplasmic poly(A) polymerase GLD-2 (Wang et al., 2002). During germ line development, the GLD-2–GLD-3 complex binds to the 3′UTR of *gld-1* mRNA and thereby regulates the rate of translation of GLD-1 protein (Suh et al., 2006). In *Drosophila*, *Bicaudal C* mutant flies develop a ‘double-abdomen’ phenotype due to ectopic expression of the posterior determinant Oskar throughout the egg (Mahone et al., 1995; Saffman et al., 1998). Molecular analysis demonstrated that Bicaudal C is required for the correct timing and localized expression of Oskar (Saffman et al., 1998), a process that is probably regulated by the interaction of Bicaudal C with the CCR4-NOT deadenylase (Chicoine et al., 2007).

At the molecular level, we propose that Bicc1 antagonizes the repressive activity of a *miR-17*-containing silencing complex that is present on the 3′UTR of *Pkd2* (Fig. 7D,D′). The nature of this antagonism remains unknown. Bicc1 could directly replace

individual proteins of the RNP silencing complex (e.g. argonaute 2; Eif2c2). Alternatively, its binding could convert the RNP complex from an inhibitory to an activating complex, as has recently been shown (Vasudevan et al., 2007). One corollary of this model is that Bicc1 does not function in a one-to-one relationship with one gene (e.g. *Pkd2*), but instead regulates multiple targets (see below). It probably recognizes its target mRNAs via an RNA interface generated by the interaction between members of the *miR-17* miRNA family and the 3′UTR. A similar scenario has recently been described for post-transcriptional regulation via the AU-rich element (ARE), in which a complex between the ARE, fragile X mental retardation 1 (FXR1) and *miR369-3* regulates a subset of target genes (Vasudevan and Steitz, 2007; Vasudevan et al., 2007). The proposed mechanism might also explain why, despite being initially described in *Drosophila* in 1986 (Mohler and Wieschaus, 1986), the function of Bicaudal C has been so difficult to define and why many attempts to identify the targets of its activity have been unsuccessful. For example, the small decrease in *Pkd2* mRNA levels in *Bicc1*$^{-/-}$ mutant mice would be disregarded in a microarray-based approach looking for twofold differences in gene expression.

This model also provided an explanation for one remaining conundrum of our present study: namely, if Pkd2 were the only target of Bicc1, the reduction of Pkd2 protein levels by ~50% should have been sufficient to cause early onset cyst formation. However, heterozygous mice lacking one copy of *Pkd2* do not show this early phenotype, but instead develop a limited number of cysts later in life (Wu et al., 2000). Similarly, if Pkd2 were the only target of Bicc1 activity, then one would expect that the complete loss of Pkd2 in *Pkd2*$^{-/-}$ mice would have a phenotypically stronger effect than the 50% reduction of Pkd2 in the *Bicc1*$^{-/-}$ mice. Therefore, Bicc1 has to regulate additional genes to cause such a strong cystic phenotype. This notion is not surprising as Bicc1 is an RNA-binding molecule and RNA-binding molecules normally regulate multiple targets. Based on our model, the presence of *miR-17* binding sites serves as a predictive tool to identify these additional targets of Bicc1. Indeed, using this bioinformatics approach we detected *miR-17* binding sites in several genes involved in PKD (see Fig. S9D in the supplementary material): *Pkd1* and *Glis3* have a highly conserved binding site, whereas *Pkhd1*, *Nek8*, *Nphp1*, *Ift88* (*Polaris*; *Tg737*) and *Nphp3* have weakly conserved sites, while a third group of genes (*Cep290*, *Hnf1b* and *Glis2*) had sites for *miR-17-3p*, a miRNA transcribed from the opposite strand of the *miR-17* precursor RNA.

Based on the presence of *miR-17* binding sites in the 3′UTR of multiple PKD genes, we would also expect to find facets of the phenotype that have still evaded detection. For example, a decrease in *Ift88* expression might result in subtle defects in ciliogenesis. However, we have not been able to detect such ciliary defects either in *Xenopus* (Tran et al., 2007) or mouse (data not shown) by immunofluorescence, but this will need a thorough analysis using electron microscopy. In addition, the *miR-17* miRNA family has been implicated in many biologically important processes, including the cell cycle and cancer, and in stem cells (Cloonan et al., 2008; Foshay and Gallicano, 2008; Mendell, 2008). Mice lacking *miR-17* family members develop a range of phenotypes, but an analysis of the kidneys is still lacking (Ventura et al., 2008). Interestingly, transgenic mice overexpressing *miR-17* show overall growth retardation, yet from all the organs analyzed, the kidneys look the most normal (Shan et al., 2009). The fact that these mice do not develop renal cysts is not surprising, as the present study proposes that one function of Bicc1 is to protect the kidney from superfluous *miR-17* activity. Instead, a cystic phenotype may only be observed once the *Bicc1* gene dose is reduced.

In conclusion, the present study reveals a novel and provocative aspect of kidney development and disease. The post-transcriptional regulation of genes involved in PKD adds a new level of complexity. *Bicc1* is, to our knowledge, the first gene to be genetically linked to this regulatory process. In addition, this study might very well spearhead similar studies in other organ systems, as it is highly unlikely that the kidney is the only organ in which post-transcriptional regulation plays such an important role.

Acknowledgements
We thank Drs S. El-Dahr, J. Larraín, T. Obara, M. Oelgeschläger and J. Venuti and all members of the laboratory for critically reviewing the manuscript and for helpful discussions; Susanne Bogusch (University of Hohenheim) for expert technical assistance; Dr P. Vize and the NIBB/NIG/NBRP *Xenopus laevis* EST project for plasmids; and Drs M. Knepper, S. Somlo and G. Wu for the Nkcc2, Pkd2, GM130 and calregulin antibodies. The anti-Lamp2 monoclonal antibody was obtained from the Developmental Studies Hybridoma Bank (DSHB) developed under the auspices of the NICHD and maintained by The University of Iowa. This work was supported by grants from the DFG to M.B. and from the Polycystic Kidney Disease Foundation (#103a2r) and NIH/NIDDK (5R21DK070671-03, 5R21DK077763-03, 1R01DK080745-01A2) to O.W. E.M.D.R. is an Investigator of the Howard Hughes Medical Institute. Deposited in PMC for release after 6 months.

Competing interests statement
The authors declare no competing financial interests.

Supplementary material
Supplementary material for this article is available at
http://dev.biologists.org/lookup/suppl/doi:10.1242/dev.046045/-/DC1

References
Agrawal, R., Tran, U. and Wessely, O. (2009). The *miR-30* miRNA family regulates *Xenopus* pronephros development and targets the transcription factor Xlim1/Lhx1. *Development* **136**, 3927-3936.
Anderson, P. and Kedersha, N. (2008). Stress granules: the Tao of RNA triage. *Trends Biochem. Sci.* **33**, 141-150.
Blum, M., Andre, P., Muders, K., Schweickert, A., Fischer, A., Bitzer, E., Bogusch, S., Beyer, T., van Straaten, H. W. and Viebahn, C. (2007). Ciliation and gene expression distinguish between node and posterior notochord in the mammalian embryo. *Differentiation* **75**, 133-146.
Burn, T. C., Connors, T. D., Dackowski, W. R., Petry, L. R., Van Raay, T. J., Millholland, J. M., Venet, M., Miller, G., Hakim, R. M., Landes, G. M. et al. (1995). Analysis of the genomic sequence for the autosomal dominant polycystic kidney disease (PKD1) gene predicts the presence of a leucine-rich repeat. The American PKD1 Consortium (APKD1 Consortium). *Hum. Mol. Genet.* **4**, 575-582.
Charlesworth, A., Cox, L. L. and MacNicol, A. M. (2004). Cytoplasmic polyadenylation element (CPE)- and CPE-binding protein (CPEB)-independent mechanisms regulate early class maternal mRNA translational activation in *Xenopus* oocytes. *J. Biol. Chem.* **279**, 17650-17659.
Chicoine, J., Benoit, P., Gamberi, C., Paliouras, M., Simonelig, M. and Lasko, P. (2007). Bicaudal-C recruits CCR4-NOT deadenylase to target mRNAs and regulates oogenesis, cytoskeletal organization, and its own expression. *Dev. Cell* **13**, 691-704.
Cloonan, N., Brown, M. K., Steptoe, A. L., Wani, S., Chan, W. L., Forrest, A. R., Kolle, G., Gabrielli, B. and Grimmond, S. M. (2008). The miR-17-5p microRNA is a key regulator of the G1/S phase cell cycle transition. *Genome Biol.* **9**, R127.
Cogswell, C., Price, S. J., Hou, X., Guay-Woodford, L. M., Flaherty, L. and Bryda, E. C. (2003). Positional cloning of jcpk/bpk locus of the mouse. *Mamm. Genome* **14**, 242-249.
Dressler, G. R. (2006). The cellular basis of kidney development. *Annu. Rev. Cell Dev. Biol.* **22**, 509-529.
Drummond, I. A. (2005). Kidney development and disease in the zebrafish. *J. Am. Soc. Nephrol.* **16**, 299-304.
Filipowicz, W., Bhattacharyya, S. N. and Sonenberg, N. (2008). Mechanisms of post-transcriptional regulation by microRNAs: are the answers in sight? *Nat. Rev. Genet.* **9**, 102-114.
Flaherty, L., Bryda, E. C., Collins, D., Rudofsky, U. and Montogomery, J. C. (1995). New mouse model for polycystic kidney disease with both recessive and dominant gene effects. *Kidney Int.* **47**, 552-558.
Foshay, K. M. and Gallicano, G. I. (2008). miR-17 family miRNAs are expressed during early mammalian development and regulate stem cell differentiation. *Dev. Biol.* **326**, 431-443.

Franks, T. M. and Lykke-Andersen, J. (2007). TTP and BRF proteins nucleate processing body formation to silence mRNAs with AU-rich elements. *Genes Dev.* **21**, 719-735.
Guay-Woodford, L. M. (2003). Murine models of polycystic kidney disease: molecular and therapeutic insights. *Am. J. Physiol.* **285**, F1034-F1049.
Hildebrandt, F., Otto, E., Rensing, C., Nothwang, H. G., Vollmer, M., Adolphs, J., Hanusch, H. and Brandis, M. (1997). A novel gene encoding an SH3 domain protein is mutated in nephronophthisis type 1. *Nat. Genet.* **17**, 149-153.
Hogan, B. L. and Kolodziej, P. A. (2002). Organogenesis: molecular mechanisms of tubulogenesis. *Nat. Rev. Genet.* **3**, 513-523.
Hughes, J., Ward, C. J., Peral, B., Aspinwall, R., Clark, K., San Millan, J. L., Gamble, V. and Harris, P. C. (1995). The polycystic kidney disease 1 (PKD1) gene encodes a novel protein with multiple cell recognition domains. *Nat. Genet.* **10**, 151-160.
Kedersha, N. and Anderson, P. (2007). Mammalian stress granules and processing bodies. *Methods Enzymol.* **431**, 61-81.
Liu, J., Rivas, F. V., Wohlschlegel, J., Yates, J. R., 3rd, Parker, R. and Hannon, G. J. (2005). A role for the P-body component GW182 in microRNA function. *Nat. Cell Biol.* **7**, 1261-1266.
Ma, W., Rogers, K., Zbar, B. and Schmidt, L. (2002). Effects of different fixatives on beta-galactosidase activity. *J. Histochem. Cytochem.* **50**, 1421-1424.
Mahone, M., Saffman, E. E. and Lasko, P. F. (1995). Localized *Bicaudal-C* RNA encodes a protein containing a KH domain, the RNA binding motif of FMR1. *EMBO J.* **14**, 2043-2055.
Maisonneuve, C., Guilleret, I., Vick, P., Weber, T., Andre, P., Beyer, T., Blum, M. and Constam, D. B. (2009). Bicaudal C, a novel regulator of Dvl signaling abutting RNA-processing bodies, controls cilia orientation and leftward flow. *Development* **136**, 3019-3030.
Markowitz, G. S., Cai, Y., Li, L., Wu, G., Ward, L. C., Somlo, S. and D'Agati, V. D. (1999). Polycystin-2 expression is developmentally regulated. *Am. J. Physiol.* **277**, F17-F25.
Mendell, J. T. (2008). miRiad roles for the miR-17-92 cluster in development and disease. *Cell* **133**, 217-222.
Mobjerg, N., Larsen, E. H. and Jespersen, A. (2000). Morphology of the kidney in larvae of Bufo viridis (Amphibia, Anura, Bufonidae). *J. Morphol.* **245**, 177-195.
Mochizuki, T., Wu, G., Hayashi, T., Xenophontos, S. L., Veldhuisen, B., Saris, J. J., Reynolds, D. M., Cai, Y., Gabow, P. A., Pierides, A. et al. (1996). PKD2, a gene for polycystic kidney disease that encodes an integral membrane protein. *Science* **272**, 1339-1342.
Mohler, J. and Wieschaus, E. F. (1986). Dominant maternal-effect mutations of *Drosophila melanogaster* causing the production of double-abdomen embryos. *Genetics* **112**, 803-822.
Nauta, J., Ozawa, Y., Sweeney, W. E., Jr, Rutledge, J. C. and Avner, E. D. (1993). Renal and biliary abnormalities in a new murine model of autosomal recessive polycystic kidney disease. *Pediatr. Nephrol.* **7**, 163-172.
Nieuwkoop, P. D. and Faber, J. (1994). *Normal Table of Xenopus laevis*. New York: Garland Publishing.
Onuchic, L. F., Furu, L., Nagasawa, Y., Hou, X., Eggermann, T., Ren, Z., Bergmann, C., Senderek, J., Esquivel, E., Zeltner, R. et al. (2002). PKHD1, the polycystic kidney and hepatic disease 1 gene, encodes a novel large protein containing multiple immunoglobulin-like plexin-transcription-factor domains and parallel beta-helix 1 repeats. *Am. J. Hum. Genet.* **70**, 1305-1317.
Parker, R. and Sheth, U. (2007). P bodies and the control of mRNA translation and degradation. *Mol. Cell* **25**, 635-646.
Pennekamp, P., Karcher, C., Fischer, A., Schweickert, A., Skryabin, B., Horst, J., Blum, M. and Dworniczak, B. (2002). The ion channel polycystin-2 is required for left-right axis determination in mice. *Curr. Biol.* **12**, 938-943.
Raciti, D., Reggiani, L., Geffers, L., Jiang, Q., Bacchion, F., Subrizi, A. E., Clements, D., Tindal, C., Davidson, D. R., Kaissling, B. et al. (2008). Organization of the pronephric kidney revealed by large-scale gene expression mapping. *Genome Biol.* **9**, R84.
Rehwinkel, J., Behm-Ansmant, I., Gatfield, D. and Izaurralde, E. (2005). A crucial role for GW182 and the DCP1:DCP2 decapping complex in miRNA-mediated gene silencing. *RNA* **11**, 1640-1647.
Saffman, E. E., Styhler, S., Rother, K., Li, W., Richard, S. and Lasko, P. (1998). Premature translation of *oskar* in oocytes lacking the RNA-binding protein Bicaudal-C. *Mol. Cell. Biol.* **18**, 4855-4862.
Saxén, L. (1987). *Organogenesis of the Kidney*. Cambridge, UK: Cambridge University Press.
Shan, S. W., Lee, D. Y., Deng, Z., Shatseva, T., Jeyapalan, Z., Du, W. W., Zhang, Y., Xuan, J. W., Yee, S. P., Siragam, V. et al. (2009). MicroRNA MiR-17 retards tissue growth and represses fibronectin expression. *Nat. Cell Biol.* **11**, 1031-1038.
Shillingford, J. M., Murcia, N. S., Larson, C. H., Low, S. H., Hedgepeth, R., Brown, N., Flask, C. A., Novick, A. C., Goldfarb, D. A., Kramer-Zucker, A. et al. (2006). The mTOR pathway is regulated by polycystin-1, and its inhibition reverses renal cystogenesis in polycystic kidney disease. *Proc. Natl. Acad. Sci. USA* **103**, 5466-5471.
Sive, H. L., Grainger, R. M. and Harland, R. M. (2000). *Early Development of Xenopus laevis: a Laboratory Manual*. Cold Spring Harbor, New York: Cold Spring Harbor Laboratory Press.
Stagner, E. E., Bouvrette, D. J., Cheng, J. and Bryda, E. C. (2009). The polycystic kidney disease-related proteins Bicc1 and SamCystin interact. *Biochem. Biophys. Res. Commun.* **383**, 16-21.
Stoecklin, G., Mayo, T. and Anderson, P. (2006). ARE-mRNA degradation requires the 5'-3' decay pathway. *EMBO Rep.* **7**, 72-77.
Suh, N., Jedamzik, B., Eckmann, C. R., Wickens, M. and Kimble, J. (2006). The GLD-2 poly(A) polymerase activates gld-1 mRNA in the Caenorhabditis elegans germ line. *Proc. Natl. Acad. Sci. USA* **103**, 15108-11512.
Sweeney, W. E., Chen, Y., Nakanishi, K., Frost, P. and Avner, E. D. (2000). Treatment of polycystic kidney disease with a novel tyrosine kinase inhibitor. *Kidney Int.* **57**, 33-40.
The International Polycystic Kidney Disease Consortium (1995). Polycystic kidney disease: the complete structure of the PKD1 gene and its protein. *Cell* **81**, 289-298.
Torres, V. E. and Harris, P. C. (2007). Polycystic kidney disease: genes, proteins, animal models, disease mechanisms and therapeutic opportunities. *J. Intern. Med.* **261**, 17-31.
Tran, U., Pickney, L. M., Ozpolat, B. D. and Wessely, O. (2007). *Xenopus* Bicaudal-C is required for the differentiation of the amphibian pronephros. *Dev. Biol.* **307**, 152-164.
Vasudevan, S. and Steitz, J. A. (2007). AU-rich-element-mediated upregulation of translation by FXR1 and Argonaute 2. *Cell* **128**, 1105-1118.
Vasudevan, S., Tong, Y. and Steitz, J. A. (2007). Switching from repression to activation: microRNAs can up-regulate translation. *Science* **318**, 1931-1934.
Ventura, A., Young, A. G., Winslow, M. M., Lintault, L., Meissner, A., Erkeland, S. J., Newman, J., Bronson, R. T., Crowley, D., Stone, J. R. et al. (2008). Targeted deletion reveals essential and overlapping functions of the miR-17 through 92 family of miRNA clusters. *Cell* **132**, 875-886.
Vize, P., Woolf, A. and Bard, J. (2002). *The Kidney: From Normal Development to Congenital Diseases*. San Diego: Academic Press.
Wang, L., Eckmann, C. R., Kadyk, L. C., Wickens, M. and Kimble, J. (2002). A regulatory cytoplasmic poly(A) polymerase in Caenorhabditis elegans. *Nature* **419**, 312-316.
Ward, C. J., Hogan, M. C., Rossetti, S., Walker, D., Sneddon, T., Wang, X., Kubly, V., Cunningham, J. M., Bacallao, R., Ishibashi, M. et al. (2002). The gene mutated in autosomal recessive polycystic kidney disease encodes a large, receptor-like protein. *Nat. Genet.* **30**, 259-269.
Wessely, O. and De Robertis, E. M. (2000). The *Xenopus* homologue of Bicaudal-C is a localized maternal mRNA that can induce endoderm formation. *Development* **127**, 2053-2062.
Wessely, O., Tran, U., Zakin, L. and De Robertis, E. M. (2001). Identification and expression of the mammalian homologue of Bicaudal-C. *Mech. Dev.* **101**, 267-270.
Wilson, P. D. and Goilav, B. (2007). Cystic Disease of the Kidney. *Ann. Rev. Path.* **2**, 341-368.
Wu, G., Markowitz, G. S., Li, L., D'Agati, V. D., Factor, S. M., Geng, L., Tibara, S., Tuchman, J., Cai, Y., Park, J. H. et al. (2000). Cardiac defects and renal failure in mice with targeted mutations in Pkd2. *Nat. Genet.* **24**, 75-78.
Xiong, H., Chen, Y., Yi, Y., Tsuchiya, K., Moeckel, G., Cheung, J., Liang, D., Tham, K., Xu, X., Chen, X. Z. et al. (2002). A novel gene encoding a TIG multiple domain protein is a positional candidate for autosomal recessive polycystic kidney disease. *Genomics* **80**, 96-104.
Zhou, X. and Vize, P. D. (2004). Proximo-distal specialization of epithelial transport processes within the *Xenopus* pronephric kidney tubules. *Dev. Biol.* **271**, 322-338.

Table S1. Distribution of the genotypes from *Bicc1*$^{+/-}$ × *Bicc1*$^{+/-}$ crosses

Bicc1 genotype	E12.5 and earlier (%)	E14.5 (%)	E15.5 (%)	E16.5 (%)	E18.5 (%)	P0/P1 (%)	P2 and older (%)
+/+	23	35	33	23	28	34	32
+/–	55	40	48	57	57	56	60
–/–	23	25	19	20	15	10	8
n	22	20	217	70	146	105	191